 DOI: 10.1002/masy.200750447

Effects of Process Conditions on Surface Replication and Higher-Order Structure Formation in Micromolding

Hiroshi Ito, Kunihiko Kazama, Takeshi Kikutani*

Summary: Injection molding of thin-wall parts with microscale surface grooves of polypropylene (PP) and cyclo-olefin copolymer (COC) were performed for this study. Effects of cavity thickness and process conditions on processability, surface replication, and higher-order structure of the molded products were evaluated. Surface replication and optical anisotropy of molded products were analyzed using a polariscope, a polarizing optical microscope, SEM, and a confocal laser scanning microscope. Optical anisotropy in the vicinity of the gate was higher than that at any other position; also, optical anisotropy increased with decreased cavity thickness. The replication property at the center area was more pronounced than those of the flow end and the gate vicinity. The distribution of the replication ratio inside the product decreased with increasing mold temperature. Results showed that the replication properties were correlated closely with skin-shear layer thickness inside the products, and that the replication ratio was lower for greater thickness of the skin-shear layer.

Keywords: injection molding; microstructure; polyolefins; structure-property relations

Introduction

Quality improvement and higher performance of molded products are strongly demanded in recent years, especially for precise and microscale products such as optical devices, medical applications, and information and communication applications. Particularly, replication of microscale or nanoscale structures is widely applicable in the field of optical applications. An intense research interest has prevailed in microscale polymer processing.[1–6] However, microscale polymer processing technology remains in a trial and error stage. For that reason and others, it is difficult to achieve an optimum product design.

Most precedent studies have restricted their scope to issues of processability and surface structure observation; the internal structure and properties of molded products have not been thoroughly examined. Molding conditions have a marked effect on structural development and final properties of molded products. Therefore, precise investigation of relationships between molding conditions and structure and physical properties is indispensable. Recently, we performed micromolding and analyzed high-order structure and final properties on micro-thin-wall molded products deeply.[7–10]

In this study, thin-wall injection moldings with microscale surface grooves were produced. Surface replication quality in transcription to microscale grooves, optical properties and internal structure of molded products were also investigated by changing the injection speed, mold wall temperature, and cavity thickness.

Experimental Part

Experiments of this study used two kinds of polymer for micromolding: a

Department of Organic and Polymeric Materials, Graduate School of Science and Engineering, Tokyo Institute of Technology, 2-12-1, O-okayama, Meguro-ku, Tokyo 152-8552, Japan
Fax: (+81) 3-5734-2876
E-mail: ihiroshi@o.cc.titech.ac.jp

semi-crystalline polymer, polypropylene (PP, MFR = 6.8 (200 °C/2.16 kg), F-704NP; Prime Polymer Co. Ltd.); and an amorphous polyolefin copolymer, cyclo-olefin copolymer (COC, Topas 6013, $T_g = 140$ °C, MVR = 13 (260 °C/2.16 kg); Ticona).

We used an intelligent analysis system for microscale injection molding, which consists of a small micro-injection molding machine, a multi-pass rheometer, and a PVT properties measurement apparatus.[7–10] For this study, a small electric injection molding machine was used for molding in this system. It has maximum clamping force, injection speed, injection pressure, injection volume of 29.4 kN, 300 mm/s, 250 MPa, and 1.4 cm^3, respectively. The machine's injection system comprises a screw barrel for plastication and a plunger injection system. The screw diameter of the plastication unit is 14 mm. An 8-mm-diameter injection plunger is employed for melt injection.

For PP molding, the injection unit temperature was 230 °C. The mold temperatures were 40 and 70 °C. On the other hand, in the case of COC molding, the temperature of the injection unit was 300 °C. The mold temperatures were 90 and 110 °C. In both cases, the injection speed was varied to 25, 50, and 150 mm/s. The holding pressure and set maximum injection pressure were, respectively, 20 and 150 MPa. In this study, the injection and packing times were 2.5 s, respectively, and the cooling time was 15 s.

The mold cavity was square with 10 mm sides, as shown in Figure 1. We prepared two kinds of lines with microscale grooves. One is a straight line parallel along the direction of melt flow. These lines are U-grooved with 300 μm pitch and: 89 μm width with 5 μm depth, 125 μm width with 10 μm depth, and 174 μm width with 20 μm depth. Each groove has 9 lines, to yield 27 lines in 9 mm square. Another shape was a grid of 800 μm in pitch, 40 μm width with 20 μm depth. At both surface patterns, the cavity thickness of the central region was varied to 0.1, 0.3 and 1.0 mm.

We investigated processability through flow length measurement of molded products using a polariscope and a digital camera. The surface replication ratio (RR) is the ratio of the depth and height of surface structures of molds and products. The replication ratio is expressed as

$$RR = {}^{h_p}/_{h_m}, \quad (1)$$

where h_p is the height of molded products, and h_m is the depth of the metal mold at each position. These depths and heights were analyzed using a scanning confocal laser microscope (SCLM, OLS1100; Olympus Optical Co. Ltd.) and a scanning electron microscope (SEM, SM-200; Topcon Corp.). We also analyzed the molecular

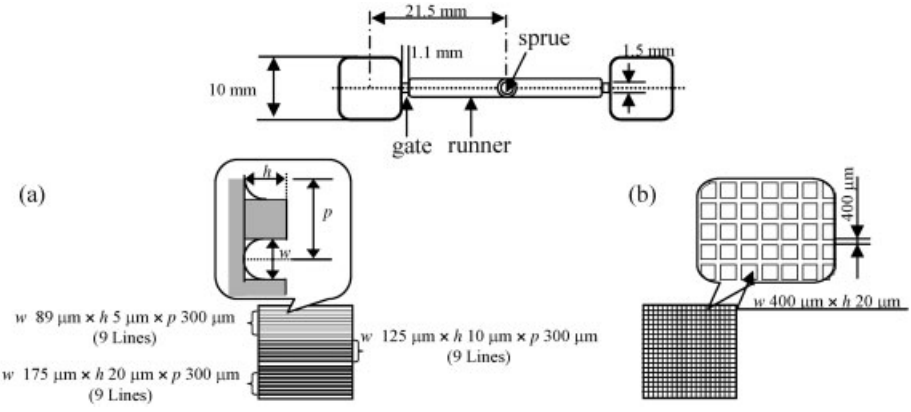

Figure 1.
Schematic diagrams of mold patterns, (a) lines and spaces (L&S) and (b) grids.

orientation of the products using a polariscope and a polarizing optical microscope (POM, BH-2; Olympus Optical Co. Ltd.) with a Berek compensator. In addition, a skin-core structure of molded products was analyzed using POM after a thin section was cut parallel to the MD from the molded products with a microtome (every 30 μm in thickness, 2055 Autocut; Leica Microsystems).

Results and Discussion

For 0.3 mm mold cavity thickness, the flow length of the product was around 10 mm for all process conditions, thereby fulfilling these conditions. On the other hand, in the case of 0.1 mm cavity thickness, the products showed short shot behavior in all conditions. The flow length decreased with decreasing cavity thickness. The cooling rate for melted resin increases when the cavity thickness decreases. At higher cooling rates, the viscosity of melted resin increases abruptly and solidification of melted resin occurs rapidly. The flow length becomes short because of increased viscosity and rapid solidification of melted resin.

We observed interference fringe patterns under a cross-polarization condition. Figure 2 shows the molded parts and a polarized photograph of COC products. The interference color was clearly visible when the injection speed increased. In addition, the interference color also became clear at low mold temperature. The interference fringe correlates closely with optical retardation.

We measured the overall optical retardation of molded products using POM with a Berek compensator. Figure 3 shows the overall optical retardation of PP and COC products at three positions: near the gate, far from the gate, and in the center of the product. Retardation was measured from the through-perspective, perpendicular to the product plane. In both products, retardation of the molded product showed a higher value in the vicinity of the gate. Retardation was also low at the flow end. Retardation increased with higher injection speed. Retardation also increased with lower mold temperature and increased cavity thickness.

Surface morphology of molded products with a grid and L&S surface pattern is shown in Figure 4. The micro structure was observed on the surface of molded products and well replicated to metal mold surface. We analyzed the surface replication properties of various molding conditions. Surface morphology and the replication ratio (RR) of PP and COC molded products with a micro-grid surface pattern are shown in Figure 5. The cavity thickness is 0.3 mm. In the direction of the polymer flow (MD), the replication ratio of PP molded product was high (ca. 95%) near the gate region, and it became lower (ca. 75%) at the flow end. On the other hand, the replication ratio of

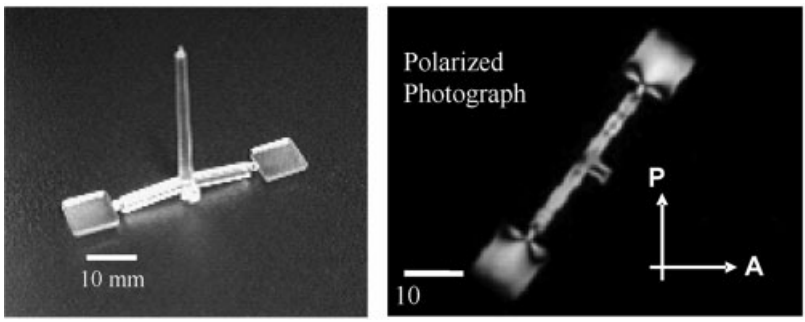

Figure 2.
Optical and polarized photographs of COC products. Cavity thickness is 0.3 mm. Injection speed is 50 mm/s and mold temperature is 90 °C.

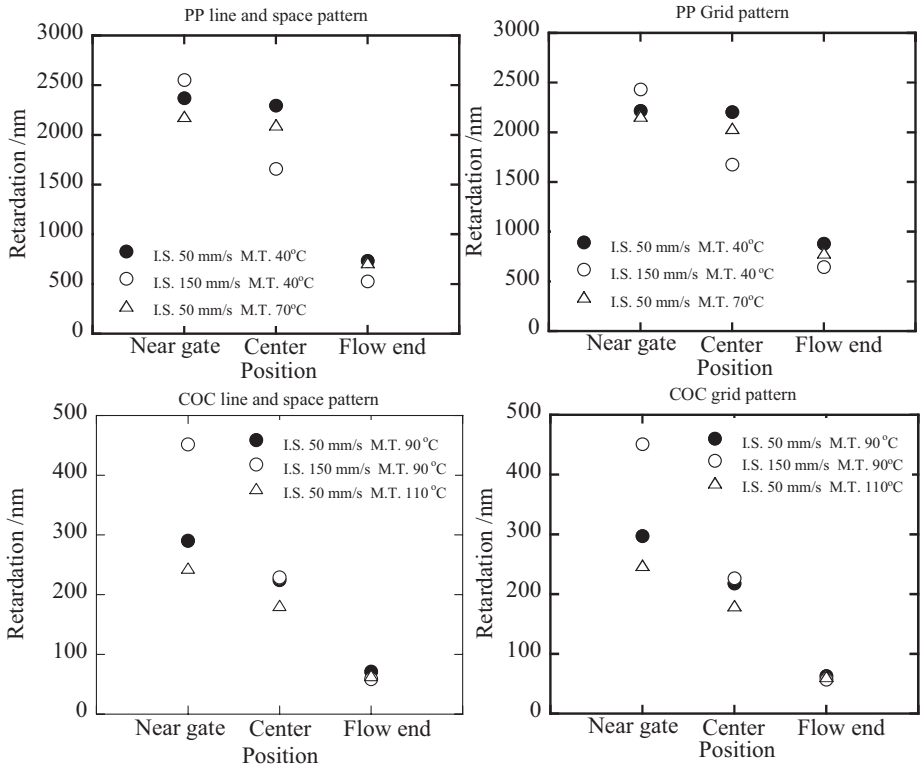

Figure 3.
Overall optical retardation of molded products. Cavity thickness is 0.3 mm. (I.S.: Injection speed, M.T.: Mold temperature).

COC molded product was high (ca. 80%) near the center region. Moreover, the ratio shows a lower value in the vicinity of gate and flow end. For higher injection speeds, the ratio was lower than that of the low injection speed in spite of the higher replication ratio at the center position. For that reason, the distribution of replication properties depends on molding conditions.

The tendency of replication properties is known to be related closely to the cavity internal pressure distribution.[11,12] At high internal pressure, molten polymer was

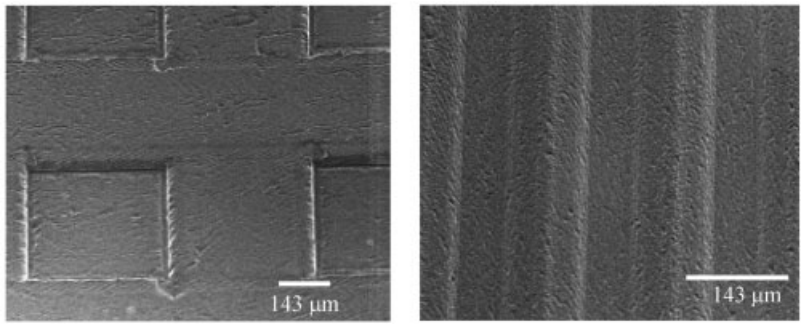

Figure 4.
SEM surface image of the grid and line&space patterns in COC products along the flow direction. Cavity thickness is 0.3 mm.

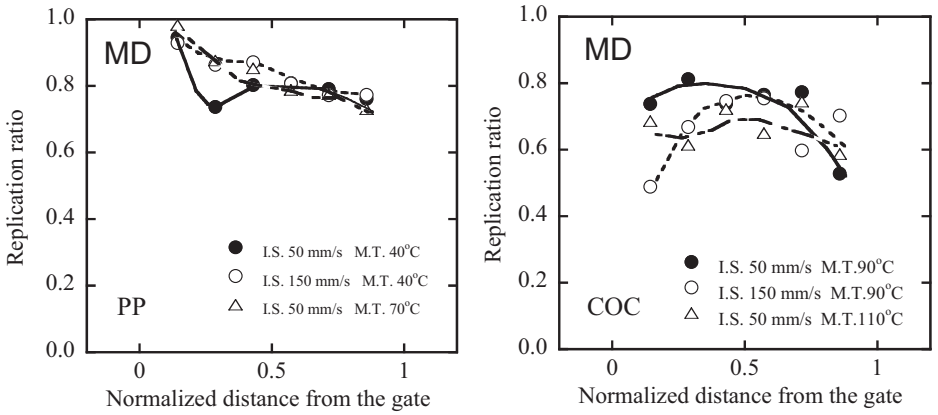

Figure 5.
Replication ratio of the grid patterns in PP and COC products along the flow direction. Cavity thickness is 0.3 mm.

generally pressed on the mold surface. Consequently, the replication ratio shows a high value near the gate and it becomes lower at the flow end. However, because the replication ratio was low near the gate, the replication properties cannot be explained merely by the pressure distribution. The injection molded product commonly has a structure distribution inside the product.[13,14] To analyze the skin-core structure and optical retardation of products with a microgrid surface, a thin section was cut parallel to the MD from the molded parts.

A cross-sectional view of the molded product with a micro-grid observed under a polarizing microscope is shown in Figure 6. The cavity thickness is 0.3 mm. Figure 7 shows local birefringence of cross-section of COC products and a schematic drawing of the extinction axis inside the convex part of the molded surface. Local birefringence showed a low value inside the convex part of products. This region corresponds to the skin layer. In the convex part, the extinction axis, which was related to molecular orientation axis, was oriented in various directions. The axis was nearly parallel to the thickness direction at the corner of the convex part, whereas the axis was oriented parallel to the polymer flow direction. Below this region, birefringence increased along the thickness direction and then decreased near the center region. The shear layer showed high birefringence values. Therefore, results confirmed a surface

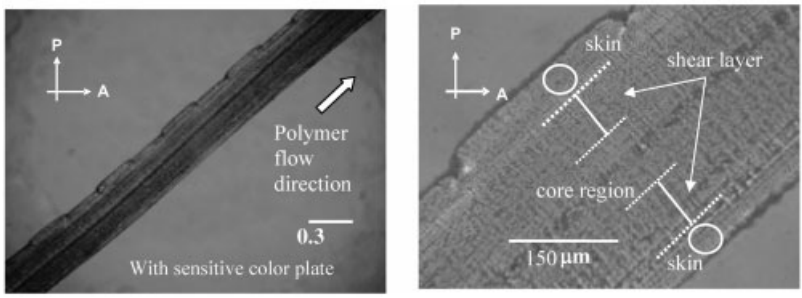

Figure 6.
Polarized microphotograph of cross-section of COC products with a micro-grid surface: cavity thickness is 0.3 mm; injection speed is 50 mm/s; mold temperature is 90 °C.

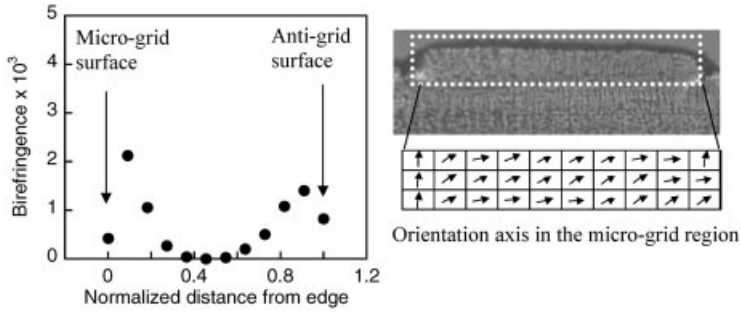

Figure 7.
Local birefringence and a schematic drawing of the extinction axis of cross-section of COC products with a micro-grid surface. Cavity thickness is 0.3 mm.

Table 1.
Thicknesses of skin and shear region of COC products.

	Skin region at micro-grid/μm	Shear layer/μm	Shear layer at anti-grid side/μm
I.S. 50 mm/s M.T. 90 °C	21	42	45
I.S. 150 mm/s M.T. 90 °C	15	61	93
I.S. 50 mm/s M.T. 110 °C	20	36	42

I.S; Injection speed, M.T.; Mold temperature.
Each position was decided at a birefringence level of 0.001.

skin-shear-core structure in the molded product. The micro-grid feature on the molded surface showed low molecular orientation: the shear region was apparent below the grid part. An inner core region with low molecular orientation was also observed. At high injection speed, the skin-shear-core structure was also observed; furthermore, the shear layer thickness was greater for products with thinner skins. The shear layer thickness was lower at high mold temperature,. For 0.3 mm COC products, we confirmed these thicknesses of the skin and shear region.

Some measurement results for skin-shear regions are shown in Table 1. These observations indicate that injection molding conditions affect the thickness of the skin and shear region. Moreover, the development of a skin-shear layer obstructed high polymer flow and addition to the internal pressure. The distribution of the replication ratio at the molded surface was influenced by the skin shear-layer thickness.

Conclusion

Thin-wall microscale injection molding with microscale grooves was carried out. Replication quality in transcription, optical properties, and internal structure of molded products were also investigated by changing the injection speed, mold wall temperature, and the cavity thickness.

Results showed that the molecular orientation in the gate vicinity was higher than these at any other position. The molecular orientation was higher with higher injection speed, and with lower mold temperature and cavity thickness. The replication property at the center position of product was higher than those

of the flow end and in the gate vicinity. Observation of cross-section of molded products confirmed a surface skin-shear-core structure in the molded product. We also observed that surface microfeatures on the molded surface showed low molecular orientation. The shear region was apparent below this area. An inner core region with low molecular orientation was observed. Surface replication properties were affected not only by pressure distribution inside the mold, but also by internal structural development. Results showed that the replication properties were correlated closely with skin-shear thickness inside the products.

Acknowledgements: This study was supported by Industrial Technology Research Grant Program in 2003, (project ID: 03A33001d) from the New Energy and Industrial Technology Development Organization (NEDO) of Japan.

[1] L. Weber, W. Ehrfeld, *Kunststoffe* **1998**, *88*, 1791.
[2] J. Zhao, R. H. Mayes, C. Ge, C. P. Sing, Conference Proceedings of PPS-18 **2002**, CD-ROM #163.
[3] S. Y. Yang, S. C. Nian, I. C. Sun, *Intern. Polymer Processing* **2002**, *XVII*, 354.
[4] B. Whiteside, M. T. Martyn, P. D. Coates, *ANTEC Tech. Papers* **2004**, 757.
[5] C. Y. Chang, S. Y. Yang, S. R. Chen, Conference Proceedings of PPS-20 **2004**, CD-ROM #121.
[6] W. Michaeli, R. Gartner, *ANTEC Tech. Papers* **2004**, 752.
[7] H. Ito, Y. Yagisawa, T. Yasuhara, T. Saito, T. Kikutani, *Theoretical Appl. Mech. Jpn.* **2005**, *LXIV*, 2511.
[8] H. Ito, Y. Yagisawa, T. Saito, T. Yasuhara, T. Kikutani, *ANTEC, Tech Papers* **2005**, *LXIII*, 894.
[9] H. Ito, K. Kazama, T. Kikutani, K. Okubo, S. Tanaka, *ANTEC, Tech Papers* **2006**, *LXIV*, 2511.
[10] H. Ito, T. Yasuhara, T. Saito, T. Kikutani, *ANTEC, Tech Papers* **2006**, *LX IV*, 2506.
[11] W. Michaeli, R. Gartner, D. Opfermann, Conference Proceedings of PPS-21 **2005**, CD-ROM #SL2-1.
[12] H. Yokoi, X. Han, Conference Proceedings of PPS-21 **2005**, CD-ROM #SL2-6.
[13] M. Fujiyama, *Polypropylene Structure, blends and Composites*, Chapman & Hall Ed., **1995**, p. 167.
[14] H. Ito, *Encyclopedia of Materials, Science and Technology*, Elsevier Science Ltd., **2001**, p. 4082.

